Lawrence Berkeley National Laboratory
LBL Publications

Title
Tribological behavior of few-nanometer-thick MoS2 prepared by low-temperature conversion of atomic layer deposited MoOx films

Permalink
https://escholarship.org/uc/item/5st2j4b2

Authors
Babuska, Tomas F
Dugger, Michael T
Walczak, Karl A
et al.

Publication Date
2023-10-01

DOI
10.1016/j.surfcoat.2023.129884

Copyright Information
This work is made available under the terms of a Creative Commons Attribution License, available at https://creativecommons.org/licenses/by/4.0/

Peer reviewed

eScholarship.org Powered by the California Digital Library
University of California

Surface & Coatings Technology 471 (2023) 129884

Contents lists available at ScienceDirect

Surface & Coatings Technology

journal homepage: www.elsevier.com/locate/surfcoat

Full length article

Tribological behavior of few-nanometer-thick MoS_2 prepared by low-temperature conversion of atomic layer deposited MoO_x films

Tomas F. Babuska [a], Michael T. Dugger [a], Karl A. Walczak [b], Ping Lu [a], Adam Schwartzberg [c], Shaul Aloni [c], Tevye R. Kuykendall [c], John F. Curry [a,*]

[a] Material, Physical and Chemical Sciences, Sandia National Laboratories, United States of America
[b] Advanced Mechanical Design, Sandia National Laboratories, United States of America
[c] The Molecular Foundry, Lawrence Berkeley National Laboratory, United States of America

ARTICLE INFO

Keywords:
MoS_2
Atomic layer deposition
Friction
Low temperature conversion

ABSTRACT

Molybdenum disulfide (MoS_2) is a popular lamellar material with desirable properties who's form, and function can vary widely, from particles to monolayer/μm thick films and applications in semiconductors to aerospace lubricants and many more. Physical vapor deposition (PVD) is commonly used to produce dense, conformal micron thick MoS_2 coatings, but lacks the ability to coat more complex geometries due to line-of-sight constraints and typically exhibit amorphous or nanocrystalline microstructures. Atomic layer deposition (ALD) has also been employed to deposit monolayer to 10's of nanometers thick lamellar solids like MoS_2 & WS_2 in transistor, sensors or electrocatalyst applications but not commonly for applications as solid lubricants in aerospace like their PVD counterparts. While recent work has shown that ALD MoS_2 can exhibit favorable microstructures for solid lubricant applications and allows for non-line of sight deposition on complex geometries, it has not been widely adopted due to high deposition temperatures (>500 °C) that can lead to softening of steel substrates. In this work, we show one of the first applications highlighting the use of ultra-thin (5–10 nm) low temperature (~250 °C) MoS_2 coatings as a promising solid lubricant for macroscale mechanical interfaces. Post-deposition chemical conversion of ALD MoO_x to MoS_2 by annealing in H_2S at temperatures ranging from 200 to 550 °C resulted in highly-ordered basally-oriented surface microstructures. The results from this work suggest that converted-ALD MoS_2 coatings can serve as viable solid lubricants for aerospace applications requiring low-temperature processing, including those with complex geometries.

1. Introduction

Molybdenum disulfide (MoS_2) is a 2D lamellar material with a wide range of applications from transistors [1], sensors [2], and electrocatalysts for the hydrogen evolution reaction [3] to low-friction ($\mu < 0.05$) solid lubricants for extreme environments such as aerospace and low-earth orbit (LEO) applications [4–6]. Often, the intended application dictates the method in which MoS_2 is deposited/grown, with chemical vapor deposition (CVD) [7,8] and atomic layer deposition (ALD) [9–11] methods used in applications requiring the opto-electronic properties of single or few-layer MoS_2 (i.e., transistors). MoS_2 coatings used as solid lubricants for mechanical and tribological applications (i.e., bearings, journals, gears) tend to be thicker (100 s of nm to micron) due to high life-cycle requirements and are deposited by mechanical burnishing/impingement [12–14] or physical vapor deposition (PVD) techniques [15–18]. Though PVD methods offer excellent thickness control and uniformity compared to mechanical burnishing/impingement, high-aspect ratio features and complex geometries can be difficult to uniformly coat with line-of-sight PVD techniques.

Conformal vapor-phase MoS_2 coating techniques (i.e., CVD, ALD) provide a unique opportunity for coating complex shapes with solid lubricants without disassembly. Recent work has demonstrated growth of MoS_2 thin films using a two-step deposition process where plasma-enhanced ALD (PE-ALD) molybdenum oxide (MoO_3) is initially deposited using an organometallic precursor like molybdenum hexacarbonyl ($Mo(CO)_6$) and O_2 plasma at low temperature (50–300 °C) followed by sulfurization in H_2S or H_2 and S at temperatures ranging from 300 to 900 °C [19–22]. Low temperature (250–325 °C) single-step thermal ALD of MoS_2 from molybdenum pentachloride ($MoCl_5$) and hydrogen sulfide (H_2S) is a common method though chlorine containing contaminants

* Corresponding author.
E-mail address: jcurry@sandia.gov (J.F. Curry).

https://doi.org/10.1016/j.surfcoat.2023.129884
Received 12 June 2023; Received in revised form 1 August 2023; Accepted 2 August 2023
Available online 6 August 2023
0257-8972/Published by Elsevier B.V. This is an open access article under the CC BY-NC-ND license (http://creativecommons.org/licenses/by-nc-nd/4.0/).

can occur in the coating [23–26]. Additionally, MoS_2 can be grown at in a single-step at low temperatures (~200 °C) through PE-ALD using Mo $(CO)_6$ and a H_2S plasma [27] though post-sulfurization at high temperatures (~600 °C) is still required improve the stoichiometry and crystallinity of the PE-ALD MoS_2 coating.

While literature has mainly focused on growth of ALD MoS_2 for applications in catalysis [28], transistors [29], and sensors [30] etc., solid lubrication using ALD MoS_2 presents a problem for materials in mechanical applications, such as bearing steels, that may potentially soften and compromise mechanical properties due to required heat treatments at high temperatures (> 500 °C) [31–33]. Though partial conversion of MoO_x to MoS_2 at low temperatures (< 500 °C) is achievable, the structure and tribological performance of ultra-thin few-nanometer ALD MoS_2 coatings as solid lubricants is not well understood and has been mainly studied at the nanoscale [34–36]. In this work, the feasibility of using low-temperature processed MoS_2 films as a solid lubricant for macroscale applications is investigated. Thin (~20 nm) MoS_2 coatings are converted from ALD grown MoO_x through sulfurization in H_2S at low temperatures from 200 to 550 °C (termed converted-ALD), and the macroscale tribological behavior and coating morphology is investigated.

2. Materials and methods

2.1. Materials synthesis

Molybdenum oxide (MoO_x) films, ~20 nm thick, were deposited on to SiO_2 coated Si substrates utilizing a Bis(t-butylimido)bis (dimethylamino)molybdenum(VI) precursor and using ALD deposition methods described previously [37]. Oxide to sulfide conversion was performed in a 4″ diameter quartz tube furnace (MTI rapid thermal processor) at 100 Torr total pressure, utilizing a flowing gas mixture of 450 sccm Ar, 50 sccm H_2, 25 sccm H_2S. The reaction temperatures were ramped (40 s ramp time) from room temperature to a annealing temperature of 200 °C, 250 °C, 300 °C, 350 °C, 450 °C and 550 °C for 1 h, then naturally cooled to room temperature under argon. Annealing temperature was varied to investigate the resulting converted-ALD coatings microstructure and tribological properties, with a goal of finding the lowest annealing temperature that will result in low friction MoS_x coatings.

2.2. Mechanical test methods

The coefficient of friction of the converted-ALD MoS_2 samples were measured using a flexure-based bidirectional reciprocating tribometer [38–40] in a dry N_2 atmosphere (O_2 & H_2O < 50 ppm). It should be noted that dry nitrogen was chosen to make assessments about intended tribological performance in vacuum because of the performance similarities between dry nitrogen and vacuum [5]. Experiments consisted of sliding for 2 mm at a velocity of 1 mm/s for 500 cycles using a 3.2 mm diameter 440C steel probe at a normal force of 100 mN (~407 MPa maximum Hertzian pressure). A minimum of three tribological experiments were performed on each sample in a new location and with a fresh counter body for repeatability. The initial coefficient of friction (termed μ_i) was calculated as the average of the first sliding cycle over each experiment. The steady-state coefficient of friction (termed μ_{ss}) was calculated for samples converted at 250–550 °C by averaging the last 200 sliding cycles of each experiment. The steady-state coefficient of friction for the 200 °C sample was calculated as the average of cycles 10–100 because the coating failed right after cycle 100.

2.3. Coating characterization

2.3.1. Focused ion beam/transmission electron microscopy

The transmission electron microscopy (TEM) cross-sections were prepared by focused ion beam (FIB), using either a protective coating consisting of e-beam platinum (Pt) or a carbon layer produced with a Sharpie™ pen [41]. The carbon layer produced with a Sharpie™ pen was used for the unannealed MoO_x sample (Fig. 1a) and samples converted at 200 °C (Fig. 1b), 250 °C (Fig. 1c) and 300 °C (Fig. 1d). Platinum was used for samples converted at 350 °C (Fig. 1e), 450 °C (Fig. 1f) and 550 °C (Fig. 1g). A FEI Titan™ G2 80–200 scanning TEM (STEM) with a Cs probe corrector and ChemiSTEM™ technology (X-FEG™ and SuperX™ EDS with four windowless silicon drift detectors) operated at 200 kV was used for structural and chemical analysis of the TEM samples. For STEM imaging, a high-angle annular dark-field (HAADF) detector with a collection range of 60–160 mrad was used. For chemical mapping, STEM energy-dispersive x-ray spectroscopy (EDS) spectral images were acquired as a series of frames, where the same region was scanned multiple times, and spatially drift-corrected to build up spectral image data. The spectral image dataset was processed [42] to yield the major components of the EDS spectra and their associated spatial concentration maps.

2.3.2. Raman spectroscopy

Raman spectra were measured on unconverted MoO_x as-deposited by ALD and converted -ALD MoS_2 samples. Raman spectra were acquired using a Horiba Yvan confocal spectrometer with a 532 nm laser, a neutral density filter of 1, 200-μm hole, grating of 1200, 100× objective, and an acquisition of 3 s with 10 integrations.

3. Results and discussion

TEM was performed on nanometer-thick MoO_x films grown on Si/SiO_2 substrates in the unconverted as-deposited state (Fig. 1a) and after annealing in H_2S at temperatures ranging from 200 to 550 °C for 1 h (Fig. 1b-g). At 200 °C, there is no observable crystalline MoS_X structure on the surface (Figs. 1b and 2a) and the formation of MoS_2 lamella appears to begin at 250 °C (Fig. 1c) where few-nanometer thick (~5 nm) basally-oriented (surface parallel lamella) crystallites (i.e., groups of individual lamella) start to form on the surface of the MoO_x. There is no noticeable crystalline structure for the 200 °C sample. However, the principal spectral components derived from analysis of the 250 °C sample's energy dispersive spectroscopy (EDS) data were used to create concentration maps of these components in the 200 °C sample (Fig. 2b), and this suggests the presence of MoS_2 on the surface (Fig. 2c).

Increasing the conversion temperature to 300 °C (Fig. 1d) and 350 °C (Fig. 1e) shows that any MoO_x converted to MoS_2 is thin (few nanometers) and surface limited with a continuous basally-oriented surface forming at 350 °C. Partial conversion of MoO_x to MoS_2 throughout the entire thickness does not start until 450 °C (Fig. 1f), indicated by MoS_2 lamella forming near the MoO_x – Si interface and around domains of MoO_x. Full conversion of the MoO_x film to MoS_2 occurs at 550 °C (Fig. 1g) with domains of basally-oriented MoS_2 crystallites near both surface and substrate as well as vertically-oriented crystallites in the bulk. The trend of increased conversion of MoO_x to MoS_2 with increasing temperature is further supported by Raman spectroscopy (Fig. 3), showing increasing intensities of the A_{1g} (out-of-plane vibration) and E_{2g} (in-plane vibration) peaks associated with MoS_2 with increasing temperature. No intensity relating to MoS_2 is observed at the 200 °C or 250 °C conversion temperature, likely due to a thin or patchy surface layer as detected by EDS (Fig. 2c). The onset of weak A_{1g} and E_{2g} peaks associated with a thin and continuous surface crystalline layer of MoS_2 (Fig. 1c) do not appear until 300 °C, which become progressively more pronounced with increasing temperature. The differences in the observed microstructures with increasing conversion temperature are likely a result of changes in the diffusion, nucleation, and reaction kinetics between H_2S, H_2, and sulfur with MoO_x. At low temperatures (200–350 °C), island growth of MoS_x clusters form through surface diffusion of precursors reacting with available Mo sites. For MoS_2, interplanar covalent bonding is more stable than intraplanar Van der Waals bonding making basal growth more energetically favorable. As

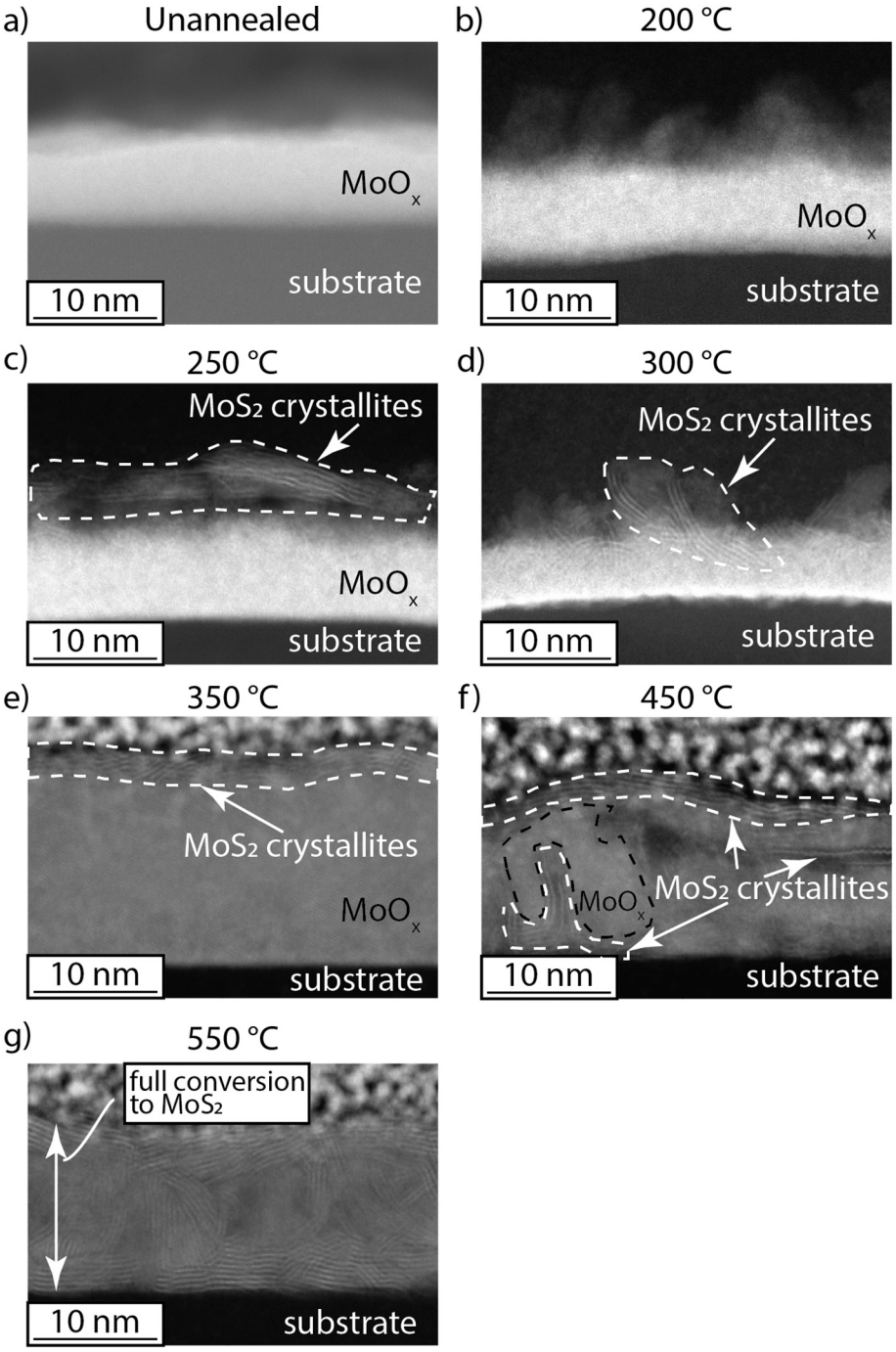

Fig. 1. (A) TEM of ALD grown MoO_x on silicon, (B) TEM of converted-ALD MoS_2, converted at 200 °C, (C) 250 °C, (D), 300 °C, (E) 350 °C, (F) 450 °C and (G) 550 °C. MoS_2 crystallites are observed on the surface after annealing MoO_x at temperatures between 250 and 350 °C and crystallites are observed to form throughout the film at 450 °C with full conversion of MoO_x to MoS_2 at 550 °C.

available Mo sites at the surface decrease, diffusion below basally-oriented surface MoS_2 drives growth deeper. With increasing conversion temperature (450–550 °C), partial conversion in the "bulk" results from diffusion pathways forming (i.e., cracks) from increased temperature driving MoO_x coarsening and reduction of the oxide. Additionally, competing growth of MoS_2 islands may cause basally-oriented crystallites to bend as they interact. As precursors are able to diffuse to the substrate-MoO_x interface, we observe basal growth possibly due to the substrate preventing vertical diffusion of precursors allowing them to diffuse along the interface, once again finding available Mo sites and nucleating basally-oriented crystallites.

The coefficient of friction was measured over 500 sliding cycles for the unconverted and converted films (Fig. 5a) and shows a dramatic reduction in both the initial (μ_i) and steady-state (μ_{ss}) coefficient of friction for all converted samples regardless of temperature when compared to the as-deposited MoO_x film. The as-deposited MoO_x coating shows an appreciably higher coefficient of friction than any of the converted films and has an increasing coefficient of friction throughout the duration of testing with a $\mu_{ss} \sim 0.8$–1 due to film failure. Annealing in H_2S for one hour at the lowest temperature sample (200 °C) decreases μ_i to 0.09 and μ_{ss} to 0.07 due to the formation of a MoS_x surface layer (Fig. 3). All samples except for the 200 °C film were able to maintain low

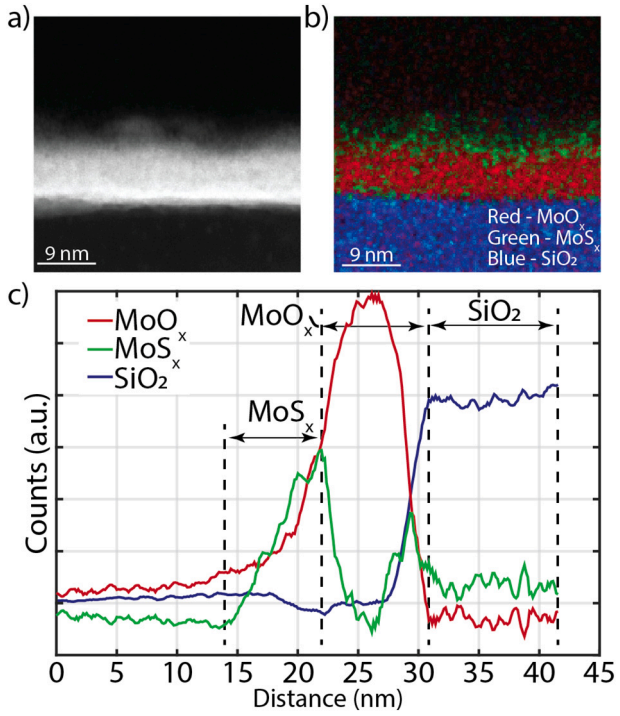

Fig. 2. (A) TEM of converted-ALD MoS_2 on silicon converted at a temperature of 200 °C and (B) the corresponding spectral image showing concentrations of MoS_x, MoO_x and SiO_2. (C) A line scan of the spectral image showing the surface does have MoS_x present even though no crystalline structure is observed.

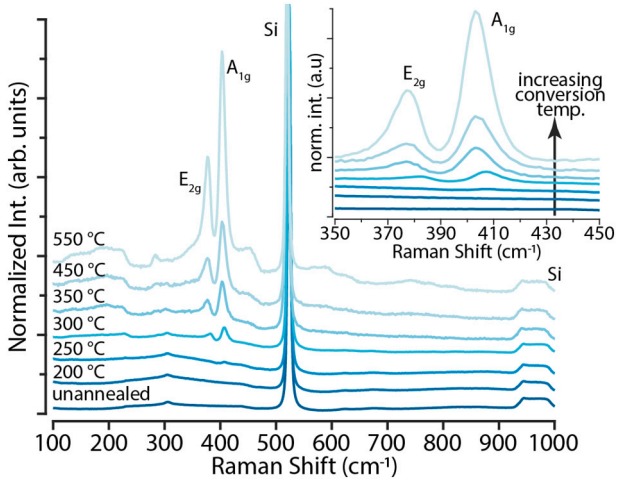

Fig. 3. Raman spectra for converted-ALD MoS_2 films converted at 200–550 °C and of the unannealed MoO_x showing increasing intensity of the A_{1g} and E_{2g} modes for MoS_2 with increasing conversion temperature.

friction throughout 500 sliding cycles with the 200 °C sample failing after ~100 sliding cycles, likely due to its limited thickness and coverage from minimal oxide conversion at such a low conversion temperature. Though μ_{ss} is nearly identical (~0.06–0.07) for all conversion temperatures (Fig. 5), the run-in behavior (transition from μ_i to μ_{ss}) and initial coefficient of friction (μ_i) changes with conversion temperature (Figs. 4b and 5) with μ_i being close to μ_{ss} at 200 °C and 250 °C and increasing above 250 °C to values between 0.1 and 0.27.

We observe that at annealing temperatures below 300 °C the initial coefficient of friction (Fig. 5) and run-in to steady-state (Fig. 4b) can be reduced due to the formation of low shear-strength basally-oriented surface MoS_2 crystallites. Due to the basally-oriented nanocrystalline nature of the converted -ALD MoS_2, the observed microstructure of the coatings (Fig. 1c-g) mimics those of mechanically-sheared MoS_2 surfaces on PVD films [43] and highly-oriented nitrogen sprayed films [12] which have been shown to decrease initial friction in both inert and humid environments and reduce oxidation susceptibility. Above annealing temperatures of 250 °C we observe an increase in both the average initial coefficient of friction and the standard deviation across all experiments (Fig. 5), which is unexpected because the amount of MoS_2 present increases (Fig. 3), and basally-oriented surfaces are observed up to the highest annealing temperature (Fig. 1g). Possible explanations of this behavior are (1) non-uniform conversion of MoO_x to MoS_2 causing regions of unconverted material, (2) the crystallite size is changing with annealing temperature and impacting initial friction through shear-strength modifications between lamellae at the sliding interface and (3) local variations in crystallite orientation causing changes in reorientation and transfer film formation at the sliding interface. TEM shows that the surface is fully converted above 350 °C (Fig. 1e), yet due to the small sample size of TEM it is possible that there are regions of unconverted material. Though possible, the position resolved friction loops of cycle 1 do not show regions of high friction suggesting that the surface is covered or that any unconverted patches are small enough to not influence the contact. Additionally, the ability for MoS_2 and MoS_2 debris in/around the contact to transfer and relubricate the contact [44] could cover higher friction unconverted regions and provide the sustained low friction observed in Fig. 4. Therefore, we expect that the surface coverage is relatively uniform and that the dependence on initial friction coefficient with annealing temperature is due to changes in crystallite size [45,46] though this hypothesis needs to be explored further in future work.

Results from the tribological testing (Figs. 4 and 5) highlight the superb lubricating properties of the ultra-thin converted-ALD MoS_2 films even at low temperature annealing in H_2S and their applications to macroscale systems. TEM (Fig. 1) shows that at temperatures below 450 °C, conversion of the top ~5–10 nm of the oxide film to MoS_2 provides low friction for hundreds of sliding cycles suggesting that the wear rates are on the order of 5×10^{-6} mm^3/Nm for the 200 °C sample (failed at ~100 cycles) to $<1 \times 10^{-6}$ mm^3/Nm for samples deposited at temperatures above 250 °C (samples did not fail after 500 cycles). The estimated wear rate range and material removal per sliding pass can be estimated using approximate contact widths using Hertzian mechanics, cycles to failure, applied normal force and film thickness as the maximum wear depth allowed before film failure (i.e., assuming no third-body contributions or relubrication from wear debris). Wear rates on the order of 5×10^{-6} mm^3/Nm equates to the removal of a single layer of MoS_2 (0.65 nm thick) for every ~3 sliding passes, while wear rates $<1 \times 10^{-6}$ mm^3/Nm mean that a single layer of MoS_2 is removed after ~16 sliding passes. The low to ultra-low wear behavior of these thin films are similar to wear resistant PVD pure and composite MoS_2 coatings typically used in macroscale applications, which have wear rates reported to vary between 1×10^{-4}–5×10^{-8} mm^3/Nm [47,48] depending on coating morphology.

Though PVD MoS_2 coatings are usually thicker (100 s of nm to micron range) than converted-ALD MoS_2, leading to longer overall lifetimes, problems arise in the deposition of micron thick coatings due to columnar growth and voiding causing low-density porous films [47,49,50] susceptible to high wear and oxidation. For low cycle applications (i.e., actuation mechanisms, latches etc.) where long duration is not a requirement, converted-ALD MoS_2 coatings are good solid lubricant candidates that will avoid issues of porosity and columnar microstructures due to the film thickness being smaller than the pore size. Furthermore, an interesting finding of this work is demonstrating how a few-nanometer thick MoO_x "bulk" does not appear to inhibit the ability for a thin MoS_x layer to provide low friction for a few hundred sliding cycles. It is possible that the oxide stabilizes the low shear-strength oriented MoS_x surface layer allowing for the low wear rate and enhances adhesion to the substrate. For PVD MoS_2 composites,

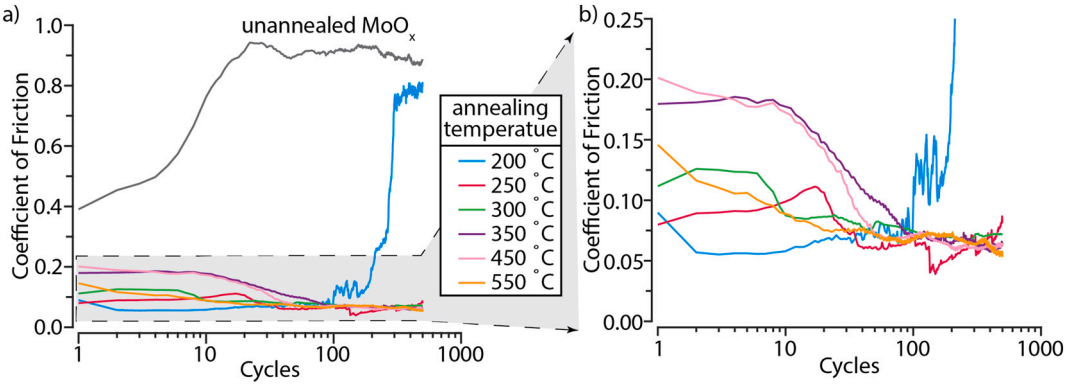

Fig. 4. (A) The average coefficient of friction of converted-ALD MoS_2 films converted at temperatures between 200 and 550 °C compared to as-deposited MoO_x and (B) a zoomed-in plot of the average coefficient showing the initial coefficient of friction, run-in behavior, and steady-state coefficient of friction.

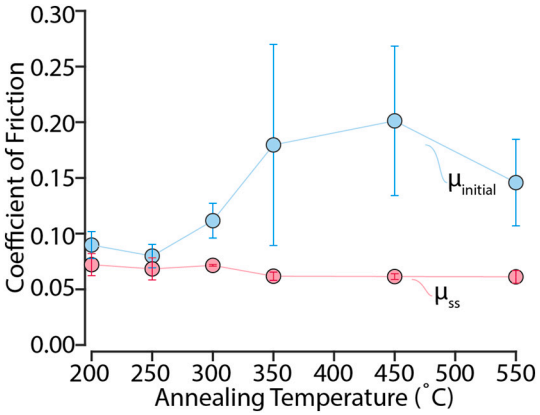

Fig. 5. Averages over 3–5 experiments of the initial coefficient of friction (μ_i) and steady-state coefficient of friction (μ_{ss}) for converted-ALD MoS_2 films converted at temperatures between 200 and 550 °C. Note: Error bars for μ_i are shown in blue while the error bars for μ_{ss} are shown in red. For some data points, the error bars are the same size as the data points and may be hard to see.

oxide dopants such as Sb_2O_3 have been shown to stabilize the sliding interface while still providing low friction [14,48,51]. For the converted-ALD coatings in this study, stabilization of the sliding interface by the oxide may potentially help provide lower wear and friction in humid environments, though this would require future work.

Highly-oriented basal microstructures, as those observed for converted-ALD MoS_2 coatings, are desirable coating morphologies for MoS_2 as they have been shown to limit oxidation from water and oxygen during storage in oxidative environments (i.e., coating aging) [13] and initial coefficients of friction [12]. Growth of basally-oriented MoS_2 microstructures with PVD methods is difficult and mechanical burnishing techniques such as nitrogen-spray impingement are the go-to leading coating manufacturing methods for highly-oriented MoS_2 solid lubricants for macroscale applications. Unlike spray impinged films, which suffer from coverage and thickness nonuniformity, low-temperature converted-ALD coatings of MoS_2 provide a new avenue to grow basally-oriented MoS_2 microstructures (Fig. 1) with macroscale applicability.

While this work has demonstrated that converted-ALD MoS_2 is a viable and promising solid lubricant for macroscale applications, longer overall coating lifetimes using micron thick films for high duty cycle applications may prove difficult for converted-ALD MoS_2 to achieve. While deposition of thick MoO_x coatings (100 s of nm) and conversion is possible, the slow growth rate of the MoO_x coating and long annealing times required to drive full conversion would likely require temperatures and times that could compromise substrate materials and be costly to deposit. A promising new avenue of converted-ALD MoS_2 would be to use it as a secondary deposition technique to PVD MoS_2 coatings to potentially grow highly-oriented surface layers on micron-thick nanocrystalline or amorphous MoS_2 coatings to improve oxidation resistance and initial coefficients of friction. Additionally, reversing the negative effects of aging, which cause surface oxidation and high coefficients of friction, using low-temperature annealing of oxidized PVD MoS_2 coatings in H_2S environments could prove a promising technique to improving the performance of conventionally processed MoS_2 coatings and should be explored in future work.

4. Conclusion

In this work, we have demonstrated that nanometer-thick (5–10 nm) converted-ALD MoS_2, prepared by converting ALD-deposited MoO_x using low-temperature annealing in H_2S, can (1) reduce the initial coefficient of friction to values <0.1 depending on conversion temperature, and (2) provide hundreds of sliding cycles of low-friction solid lubrication with steady-state coefficients of friction on the order of ~0.06–0.07. We show that annealing MoO_x at 250 °C for 1 h in H_2S is the lowest temperature that can still provide low initial friction (μ_i ~ 0.08) and steady-state friction (μ_{ss} ~ 0.07) for 500 sliding cycles. While complete conversion of the MoO_x coating is achieved at 550 °C, we find that annealing at 250 °C results in only the top ~5 nm of the MoO_x coating having been converted to MoS_2 and that this ultra-thin layer is able to provide macroscale lubrication comparable to micron-thick PVD processed MoS_2 coatings. This work has shown that utilizing low-temperature nanometer-thick converted-ALD MoS_2 as a solid lubricant coating for mechanical interfaces overcomes two limitations of other deposition techniques such as PVD and high-temperature CVD/ALD: (1) growth temperatures above 500 °C can soften load bearing steels (such as bearing steels) compromising the integrity of the mechanical components, and (2) coating complex geometries with high-aspect ratio features, such as gears, results in large variability in thickness with location on the part due to shadowing.

CRediT authorship contribution statement

Tomas F. Babuska: Writing – Original Draft, Data Curation, Writing – Review & Editing, Visualization, Investigation. **Michael T. Dugger**: Writing – Original Draft, Writing – Review & Editing, Conceptualization, Funding Acquisition, Project Management. **Karl A. Walczak:** Conceptualization, Writing – Review & Editing, Conceptualization. **Ping Lu:** Methodology, Formal Analysis, Writing – Review & Editing, Investigation. **Adam Schwartzberg:** Project Administration, Resources, Methodology. **Shaul Aloni:** Project Administration, Resources, Methodology. **Tevye R. Kuykendall:** Writing – Review & Editing, Formal Analysis,

Investigation, Resources. **John F. Curry:** Writing – Original Draft, Data Curation, Writing – Review & Editing, Funding Acquisition, Project Management, Supervision, Conceptualization.

Declaration of competing interest

The authors declare that they have no known competing financial interests or personal relationships that could have appeared to influence the work reported in this paper.

Data availability

Data will be made available on request.

Acknowledgements

This work was funded by the Laboratory Directed Research and Development (LDRD) program at Sandia National Laboratories, a multi-mission laboratory managed and operated by National Technology and Engineering Solutions of Sandia, LLC., a wholly owned subsidiary of Honeywell International, Inc., for the U.S. Department of Energy's National Nuclear Security Administration under contract DE-NA0003525. Work at the Molecular Foundry was supported by the Office of Science, Office of Basic Energy Sciences, of the U.S. Department of Energy under Contract No. DE-AC02-05CH11231. This paper describes objective technical results and analysis. Any subjective views or opinions that might be expressed in the paper do not necessarily represent the views of the U.S. Department of Energy or the United States Government.

References

[1] A. Bala, N. Liu, A. Sen, Y. Cho, P. Pujar, B. So, S. Kim, Low-temperature plasma-assisted growth of large-area MoS $_2$ for transparent phototransistors, Adv. Funct. Mater. 32 (2022) 2205106.
[2] C. Ahn, J. Lee, H.-U. Kim, H. Bark, M. Jeon, G.H. Ryu, Z. Lee, G.Y. Yeom, K. Kim, J. Jung, Y. Kim, C. Lee, T. Kim, Low-temperature synthesis of large-scale molybdenum disulfide thin films directly on a plastic substrate using plasma-enhanced chemical vapor deposition, Adv. Mater. 27 (2015) 5223–5229.
[3] N. Liu, J. Kim, J. Oh, Q.T. Nguyen, B.B. Sahu, J.G. Han, S. Kim, Growth of multiorientated polycrystalline MoS2 using plasma-enhanced chemical vapor deposition for efficient hydrogen evolution reactions, Nanomaterials (Basel) 10 (2020), https://doi.org/10.3390/nano10081465.
[4] M.R. Hilton, P.D. Fleischauer, Applications of solid lubricant films in spacecraft, Surf. Coat. Technol. 54–55 (1992) 435–441.
[5] C. Donnet, J.M. Martin, T. Le Mogne, M. Belin, Super-low friction of MoS2 coatings in various environments, Tribol. Int. 29 (1996) 123–128.
[6] T. Le Mogne, C. Donnet, J.M. Martin, A. Tonck, N. Millard-Pinard, S. Fayeulle, N. Moncoffre, Nature of super-lubricating MoS2 physical vapor deposition coatings, J. Vac. Sci. Technol. A 12 (1994) 1998–2004.
[7] H.F. Liu, S.L. Wong, D.Z. Chi, CVD growth of MoS2-based two-dimensional materials, Chem. Vap. Depos. 21 (2015) 241–259.
[8] J.C. Kotsakidis, Q. Zhang, A.L. Vazquez de Parga, M. Currie, K. Helmerson, D. K. Gaskill, M.S. Fuhrer, Oxidation of monolayer WS2 in ambient is a Photoinduced process, Nano Lett. 19 (2019) 5205–5215.
[9] A. Valdivia, D.J. Tweet, J.F. Conley, Atomic layer deposition of two dimensional MoS2 on 150 mm substrates, J. Vac. Sci. Technol. A 34 (2016), 021515.
[10] Y. Jang, S. Yeo, H.-B.-R. Lee, H. Kim, S.-H. Kim, Wafer-scale, conformal and direct growth of MoS2 thin films by atomic layer deposition, Appl. Surf. Sci. 365 (2016) 160–165.
[11] J.J. Pyeon, S.H. Kim, D.S. Jeong, S.-H. Baek, C.-Y. Kang, J.-S. Kim, S.K. Kim, Wafer-scale growth of MoS2 thin films by atomic layer deposition, Nanoscale 8 (2016) 10792–10798.
[12] J.F. Curry, N. Argibay, T. Babuska, B. Nation, A. Martini, N.C. Strandwitz, M. T. Dugger, B.A. Krick, Highly oriented MoS2 coatings: tribology and environmental stability, Tribol. Lett. 64 (2016) 11.
[13] J.F. Curry, M.A. Wilson, H.S. Luftman, N.C. Strandwitz, N. Argibay, M. Chandross, M.A. Sidebottom, B.A. Krick, Impact of microstructure on MoS2 oxidation and friction, ACS Appl. Mater. Interfaces 9 (2017) 28019–28026.
[14] J.S. Zabinski, J.E. Bultman, J.H. Sanders, J.J. Hu, Multi-environmental lubrication performance and lubrication mechanism of MoS2/Sb2O3/C composite films, Tribol. Lett. 23 (2006) 155–163.
[15] T. Spalvins, Morphological and frictional behavior of sputtered MoS2 films, Thin Solid Films 96 (1982) 17–24.
[16] T. Spalvins, Tribological properties of sputtered MoS2 films in relation to film morphology, Thin Solid Films 73 (1980) 291–297.
[17] M.R. Hilton, R. Bauer, P.D. Fleischauer, Tribological performance and deformation of sputter-deposited MoS2 solid lubricant films during sliding wear and indentation contact, Thin Solid Films 188 (1990) 219–236.
[18] V. Buck, Preparation and properties of different types of sputtered MoS2 films, Wear. 114 (1987) 264–274.
[19] M. Demirtaş, C. Odacı, Y. Shehu, N.K. Perkgöz, F. Ay, Layer and size distribution control of CVD-grown 2D MoS2 using ALD-deposited MoO3 structures as the precursor, Mater. Sci. Semicond. Process. 108 (2020), 104880.
[20] C. Martella, P. Melloni, E. Cinquanta, E. Cianci, M. Alia, M. Longo, A. Lamperti, S. Vangelista, M. Fanciulli, A. Molle, Engineering the growth of MoS2via atomic layer deposition of molybdenum oxide film precursor, Adv. Electron. Mater. 2 (2016) 1600330.
[21] B.D. Keller, A. Bertuch, J. Provine, G. Sundaram, N. Ferralis, J.C. Grossman, Process control of atomic layer deposition molybdenum oxide nucleation and sulfidation to large-area MoS2 monolayers, Chem. Mater. 29 (2017) 2024–2032.
[22] A. Sharma, R. Mahlouji, L. Wu, M.A. Verheijen, V. Vandalon, S. Balasubramanyam, J.P. Hofmann, W.M. (Erwin) Kessels, A.A. Bol, Large area, patterned growth of 2D MoS2 and lateral MoS2–WS2 heterostructures for nano- and opto-electronic applications, Nanotechnology 31 (2020), 255603.
[23] J. Yang, L. Liu, Trickle flow aided atomic layer deposition (ALD) strategy for ultrathin molybdenum disulfide (MoS2) synthesis, ACS Appl. Mater. Interfaces 11 (2019) 36270–36277.
[24] Y. Kim, J.-G. Song, Y.J. Park, G.H. Ryu, S.J. Lee, J.S. Kim, P.J. Jeon, C.W. Lee, W. J. Woo, T. Choi, H. Jung, H.-B.-R. Lee, J.-M. Myoung, S. Im, Z. Lee, J.-H. Ahn, J. Park, H. Kim, Self-limiting layer synthesis of transition metal dichalcogenides, Sci. Rep. 6 (2016) 18754.
[25] T.A. Ho, C. Bae, S. Lee, M. Kim, J.M. Montero-Moreno, J.H. Park, H. Shin, Edge-on MoS2 thin films by atomic layer deposition for understanding the interplay between the active area and hydrogen evolution reaction, Chem. Mater. 29 (2017) 7604–7614.
[26] J. Joe, C. Bae, E. Kim, T.A. Ho, H. Yang, J.H. Park, H. Shin, Mixed-phase (2H and 1T) MoS2 catalyst for a highly efficient and stable Si photocathode, Catalysts 8 (2018) 580.
[27] S. Oh, J.B. Kim, J.T. Song, J. Oh, S.-H. Kim, Atomic layer deposited molybdenum disulfide on Si photocathodes for highly efficient photoelectrochemical water reduction reaction, J. Mater. Chem. A Mater. Energy Sustain. 5 (2017) 3304–3310.
[28] C.C.L. McCrory, S. Jung, I.M. Ferrer, S.M. Chatman, J.C. Peters, T.F. Jaramillo, Benchmarking hydrogen evolving reaction and oxygen evolving reaction electrocatalysts for solar water splitting devices, J. Am. Chem. Soc. 137 (2015) 4347–4357.
[29] S.B. Desai, S.R. Madhvapathy, A.B. Sachid, J.P. Llinas, Q. Wang, G.H. Ahn, G. Pitner, M.J. Kim, J. Bokor, C. Hu, H.-S.P. Wong, A. Javey, MoS2 transistors with 1-nanometer gate lengths, Science 354 (2016) 99–102.
[30] H. Long, A. Harley-Trochimczyk, T. Pham, Z. Tang, T. Shi, A. Zettl, C. Carraro, M. A. Worsley, R. Maboudian, High surface area MoS2/graphene hybrid aerogel for ultrasensitive NO2Detection, Adv. Funct. Mater. 26 (2016) 5158–5165.
[31] P.W. Hochanadel, G.R. Edwards, C.V. Robino, M.J. Cieslak, Heat treatment of investment cast PH 13-8 Mo stainless steel: part I. mechanical properties and microstructure, Metall. Mater. Trans. A. 25 (1994) 789–798.
[32] Z. Huang, Abad, J.K. Ramsey, M.R. Figueiredo de, D. Kaoumi, N. Li, M. Asta, N. Gronbech-Jensen, P. Hosemann, A high temperature mechanical study on PH 13-8 Mo maraging steel, Mater. Sci. Eng. A 651 (2016) 574–582.
[33] V. Seetharaman, M. Sundararaman, R. Krishnan, Precipitation hardening in a PH 13-8 Mo stainless steel, Mater. Sci. Eng. 47 (1981) 1–11.
[34] J. Yang, L. Liu, Nanotribological properties of 2-D MoS2 on different substrates made by atomic layer deposition (ALD), Appl. Surf. Sci. 502 (2020), 144402.
[35] J. Yang, X. Xu, L. Liu, Plasma-assisted friction control of 2D MoS2 made by atomic layer deposition, Nanotechnology. 31 (2020), 395711.
[36] Y. Huang, L. Liu, J. Lv, J. Yang, J. Sha, Y. Chen, MoS2 solid-lubricating film fabricated by atomic layer deposition on Si substrate, AIP Adv. 8 (2018), 045216.
[37] C.T. Chen, J. Pedrini, E.A. Gaulding, C. Kastl, G. Calafiore, S. Dhuey, T. R. Kuykendall, S. Cabrini, F.M. Toma, S. Aloni, A.M. Schwartzberg, Very high refractive index transition metal dichalcogenide photonic conformal coatings by conversion of ALD metal oxides, Sci. Rep. 9 (2019) 2768.
[38] B.A. Krick, J.R. Vail, B.N.J. Persson, W.G. Sawyer, Optical in situ Micro Tribometer for analysis of real contact area for contact mechanics, adhesion, and sliding experiments, Tribol. Lett. 45 (2012) 185–194.
[39] D.L. Burris, W.G. Sawyer, Addressing practical challenges of low friction coefficient measurements, Tribol. Lett. 35 (2009) 17–23.
[40] R.S. Colbert, B.A. Krick, A.C. Dunn, J.R. Vail, N. Argibay, W.G. Sawyer, Uncertainty in pin-on-disk wear volume measurements using surface scanning techniques, Tribol. Lett. 42 (2011) 129–131.
[41] Y.C. Park, B.C. Park, S. Romankov, K.J. Park, J.H. Yoo, Y.B. Lee, J.-M. Yang, Use of permanent marker to deposit a protection layer against FIB damage in TEM specimen preparation, J. Microsc. 255 (2014) 180–187.
[42] P.G. Kotula, M.R. Keenan, J.R. Michael, Automated analysis of SEM X-ray spectral images: a powerful new microanalysis tool, Microsc. Microanal. 9 (2003) 1–17.
[43] T.F. Babuska, J.F. Curry, M.T. Dugger, P. Lu, Y. Xin, S. Klueter, A.C. Kozen, T. Grejtak, B.A. Krick, Role of environment on the shear-induced structural evolution of MoS2 and impact on oxidation and tribological properties for space applications, ACS Appl. Mater. Interfaces 14 (2022) 13914–13924.
[44] K.J. Wahl, I.L. Singer, Quantification of a lubricant transfer process that enhances the sliding life of a MoS2 coating, Tribol. Lett. 59–66 (1995).
[45] J.F. Curry, T. Ohta, F.W. DelRio, P. Mantos, M.R. Jones, T.F. Babuska, N.S. Bobbitt, N. Argibay, B.A. Krick, M.T. Dugger, M. Chandross, Structurally driven environmental degradation of friction in MoS2 films, Tribol. Lett. 69 (2021) 96.

[46] P.D. Fleischauer, R. Bauer, Chemical and structural effects on the lubrication properties of sputtered MoS2 films, Tribol. Trans. 31 (1988) 239–250.
[47] T.F. Babuska, J.F. Curry, M.T. Dugger, M.R. Jones, F.W. DelRio, P. Lu, Y. Xin, T. Grejtak, R. Chrostowski, F. Mangolini, N.C. Strandwitz, M.I. Chowdhury, G. L. Doll, B.A. Krick, Quality control metrics to assess MoS2 sputtered films for tribological applications, Tribol. Lett. 70 (2022), https://doi.org/10.1007/s11249-022-01642-y.
[48] T.W. Scharf, P.G. Kotula, S.V. Prasad, Friction and wear mechanisms in MoS2/Sb2O3/Au nanocomposite coatings, Acta Mater. 58 (2010) 4100–4109.
[49] A. Seynstahl, S. Krauß, E. Bitzek, B. Meyer, B. Merle, S. Tremmel, Microstructure, mechanical properties and tribological behavior of magnetron-sputtered MoS2 solid lubricant coatings deposited under industrial conditions, Coatings (2021), https://doi.org/10.3390/coatings11040455.
[50] V. Buck, Structure and density of sputtered MoS2 films, Vacuum 36 (1986) 89–94.
[51] J.S. Zabinski, M.S. Donely, N.T. McDevitt, Mechanistic study of the synergism between Sb203 and MoS2 lubricant systems using Raman spectroscopy, Wear 103–108 (1993).